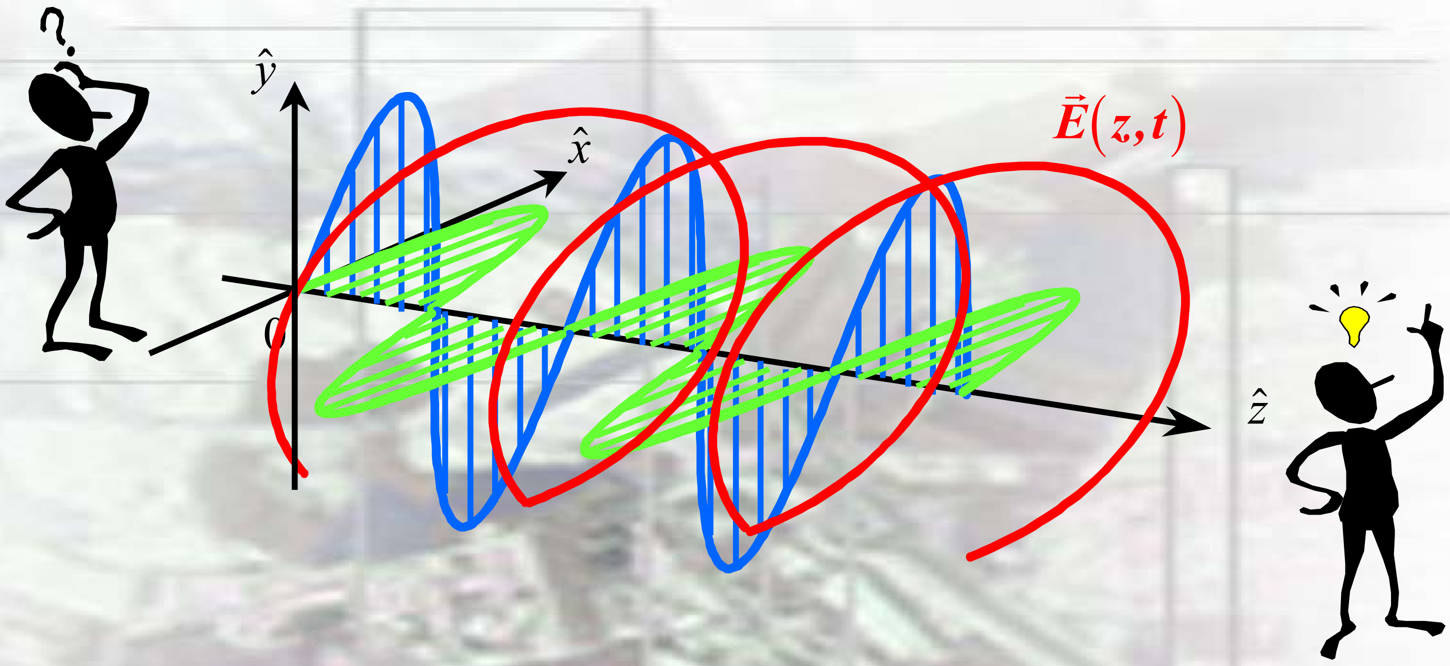

POL-IN-SAR CLASSIFICATION

POLARIMETRIC REMOTE SENSING

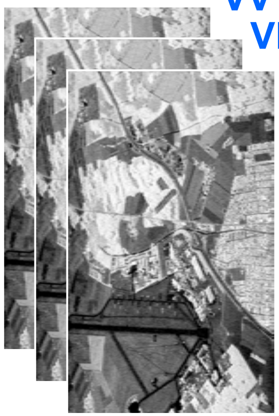

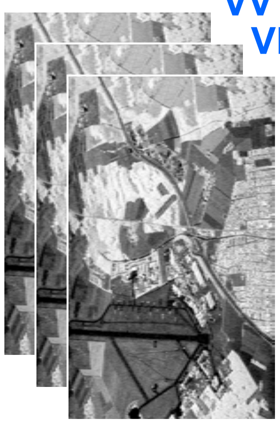

WISHART PDF

$$P(\langle[T]\rangle/[T_m]) = \frac{L^{Lp}\,|\langle[T]\rangle|^{L-p}\,e^{-LTr([T_m]^{-1}\langle[T]\rangle)}}{\pi^{\frac{p(p-1)}{2}}\,\Gamma(L)\ldots\Gamma(L-p+1)\,|[T_m]|^{L}}$$

POLINSAR CLASSIFICATION

L. FERRO-FAMIL, E.POTTIER, J.S LEE (2002)

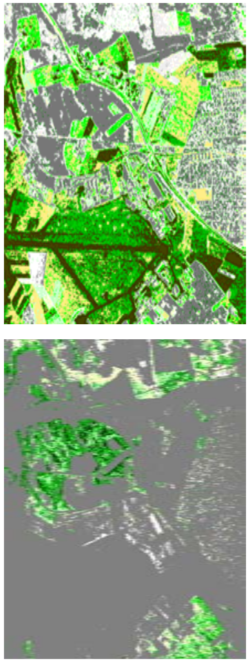

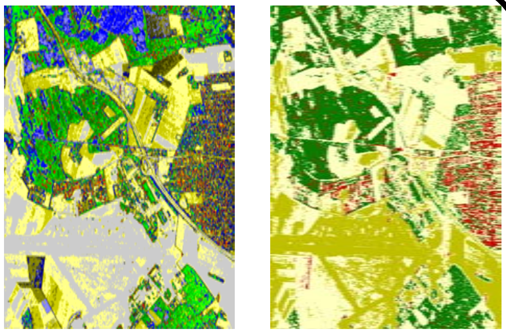

POLSAR CLASSIFICATION

OPTIMUM INTERFEROMETRIC COHERENCES SPECTRUM

DUAL-CHANNELS CLASSIFICATION

POLSAR

INSAR

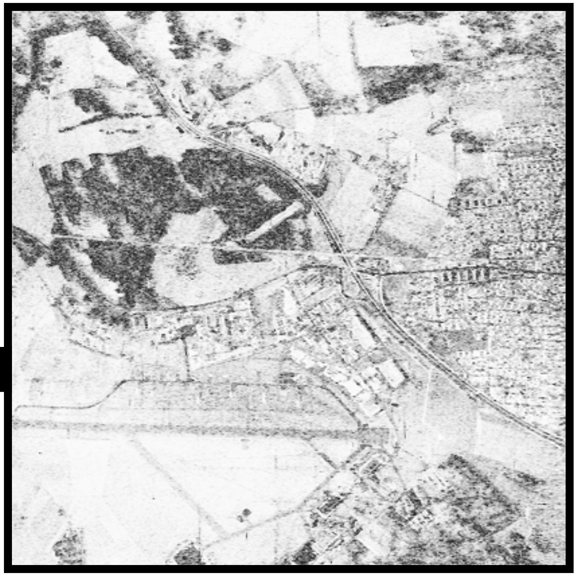

POL-IN-SAR CLASSIFICATION

POLINSAR – WISHART CLASSIFIER

L. Ferro-Famil, E. Pottier, J.S. Lee (2001-2002)

POLARIMETRY AND INTERFEROMETRY

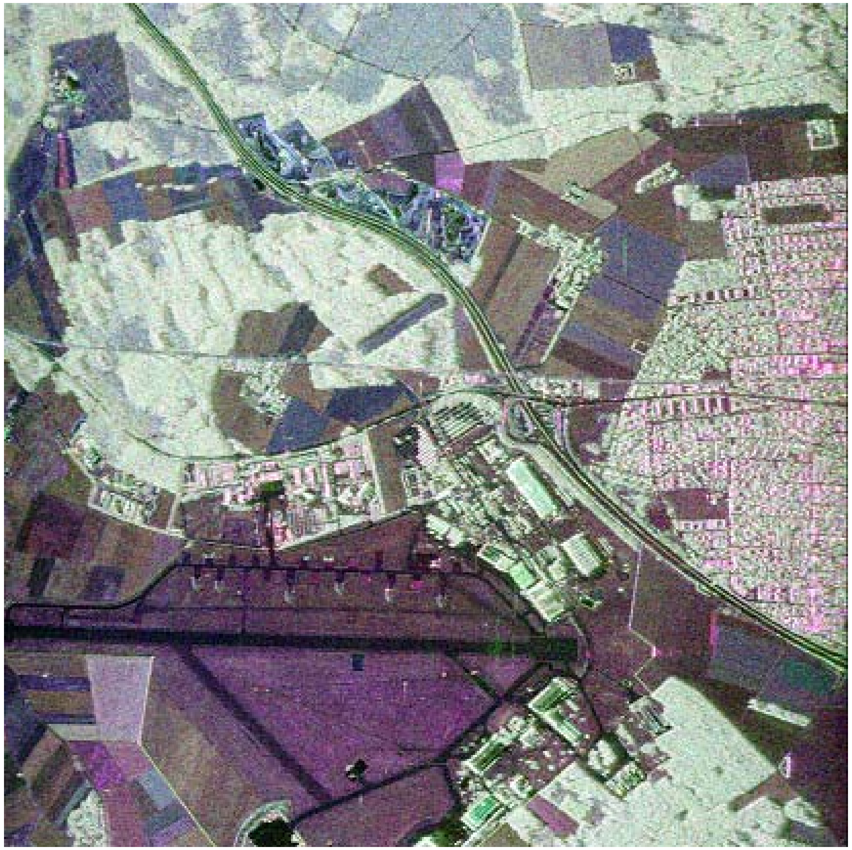

DLR E-SAR L Band
In-Pol SAR (1.5m x 3m) – Baseline 5m

POL-SAR INFORMATION

IN-SAR INFORMATION γ

COMPLEMENTARY INFORMATION

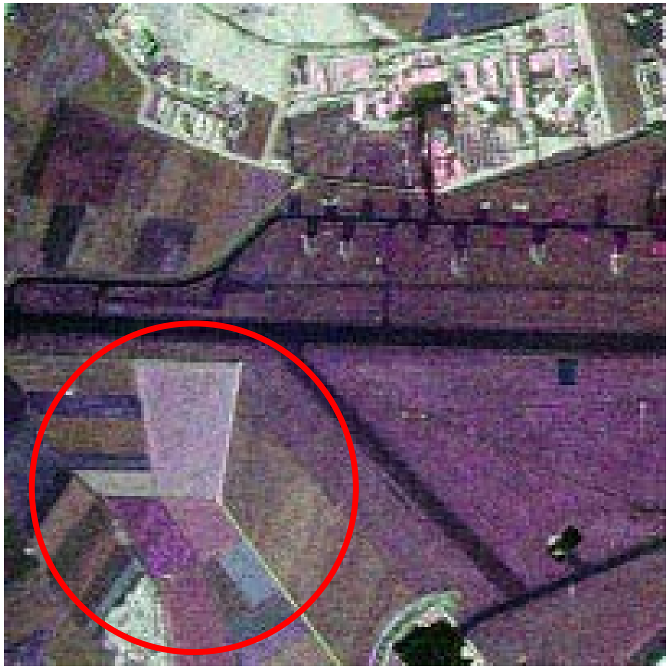

HETEROGENEOUS AREA

DIFFERENT POLARIMETRIC SCATTERING MECHANISMS

HOMOGENEOUS AREA

CONSTANT INTERFEROMETRIC COHERENCE

POLARIMETRY AND INTERFEROMETRY

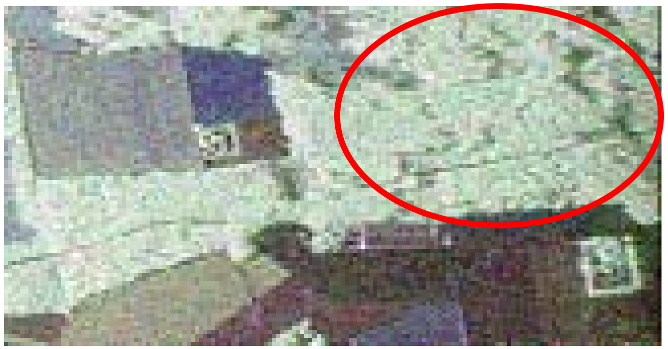

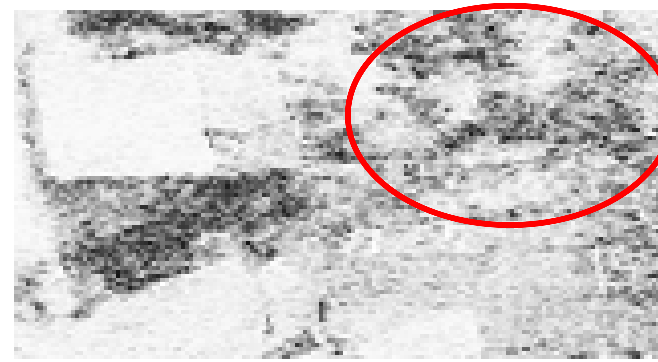

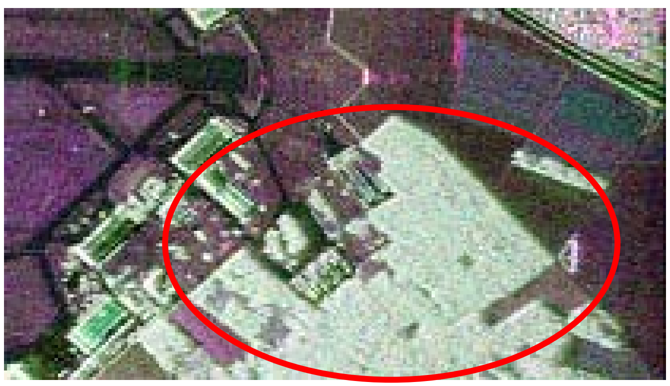

HOMOGENEOUS AREA

SAME POLARIMETRIC SCATTERING MECHANISMS

HETEROGENEOUS AREA

DIFFERENT INTERFEROMETRIC COHERENCE

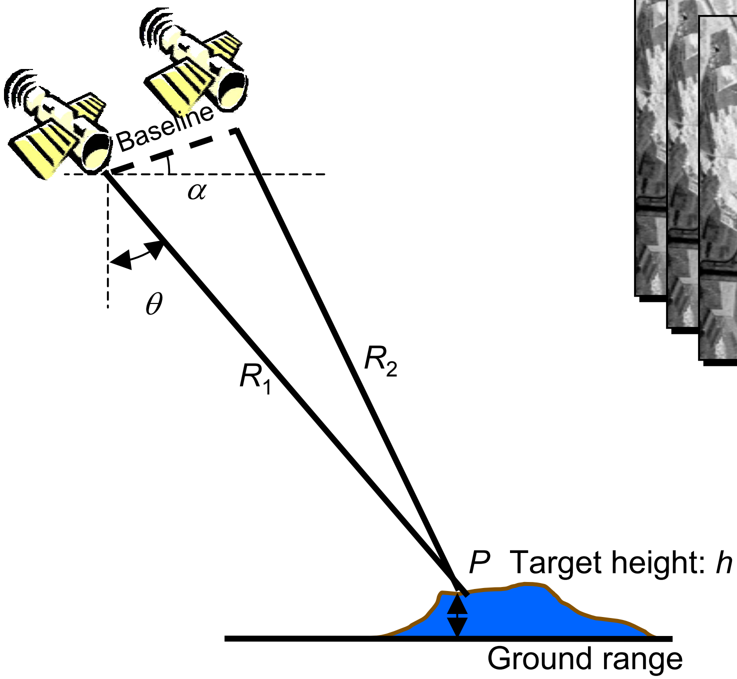

$$\underline{k}_1 = \frac{1}{\sqrt{2}}\begin{bmatrix} S_{XX_1} + S_{YY_1} \\ S_{XX_1} - S_{YY_1} \\ 2S_{XY_1} \end{bmatrix}$$

$$\underline{\underline{k}} = \begin{bmatrix} \underline{k}_1 \\ \underline{k}_2 \end{bmatrix}$$

POLARIMETRIC INTERFEROMETRIC TARGET VECTOR

$$\underline{k}_2 = \frac{1}{\sqrt{2}}\begin{bmatrix} S_{XX_2} + S_{YY_2} \\ S_{XX_2} - S_{YY_2} \\ 2S_{XY_2} \end{bmatrix}$$

$$\underline{\underline{k}} = \begin{bmatrix} \underline{k}_1 \\ \underline{k}_2 \end{bmatrix}$$

POLARIMETRIC INTERFEROMETRIC TARGET VECTOR

$$\langle [T_6] \rangle = \langle \underline{\underline{k}} \cdot \underline{\underline{k}}^{T*} \rangle = \begin{bmatrix} \langle \underline{k}_1 \cdot \underline{k}_1^{T*} \rangle & \langle \underline{k}_1 \cdot \underline{k}_2^{T*} \rangle \\ \langle \underline{k}_2 \cdot \underline{k}_1^{T*} \rangle & \langle \underline{k}_2 \cdot \underline{k}_2^{T*} \rangle \end{bmatrix} = \begin{bmatrix} \langle [T_1] \rangle & \langle [\Omega_{12}] \rangle \\ \langle [\Omega_{12}]^{T*} \rangle & \langle [T_2] \rangle \end{bmatrix}$$

POLARIMETRIC INTERFEROMETRIC COHERENCY MATRIX (6x6)

$\langle [T_1] \rangle$ HERMITIAN POLARIMETRIC COHERENCY MATRIX (3x3)

$\langle [T_2] \rangle$ HERMITIAN POLARIMETRIC COHERENCY MATRIX (3x3)

$\langle [\Omega_{12}] \rangle$ NON HERMITIAN POLARIMETRIC INTER-COHERENCY MATRIX (3x3)

POLARIMETRY AND INTERFEROMETRY

POLSAR IMAGES $I_1 = \underline{w}_1^{T*} \cdot \underline{k}_1$ and $I_2 = \underline{w}_2^{T*} \cdot \underline{k}_2$

With: $(\underline{w}_1, \underline{w}_2)$ **Complex Unitary Vectors**

⬇

$$\gamma(\underline{w}_1, \underline{w}_2) = \frac{\langle I_1 I_2^* \rangle}{\sqrt{\langle I_1 I_1^* \rangle \langle I_2 I_2^* \rangle}} = \frac{\langle \underline{w}_1 [\Omega_{12}] \underline{w}_2^{T*} \rangle}{\sqrt{\langle \underline{w}_1 [T_1] \underline{w}_1^{T*} \rangle \langle \underline{w}_2 [T_2] \underline{w}_2^{T*} \rangle}}$$

COMPLEX POLARIMETRIC INTERFEROMETRIC COHERENCE

$arg(\gamma)$ **INTERFEROMETRIC PHASE**

$|\gamma|$ **CROSS-CORRELATION COEFFICIENT**

$$\gamma = \gamma_{SNR} \cdot \gamma_{spatial} \cdot \gamma_{temporal} \cdot \gamma_{polar}$$

POLARIMETRY AND INTERFEROMETRY

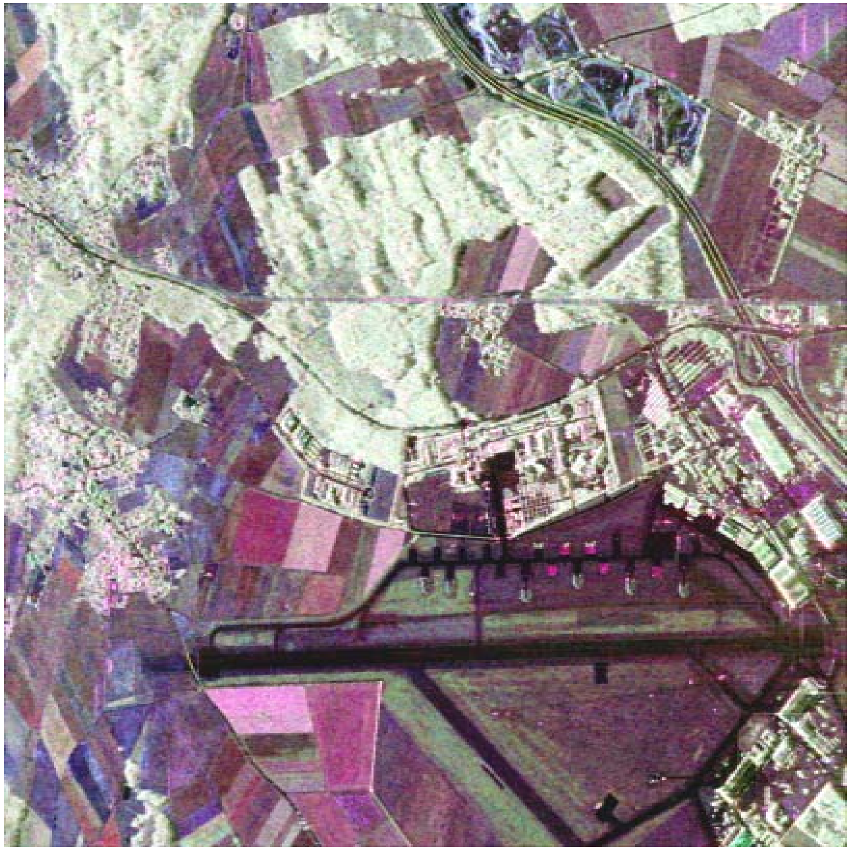

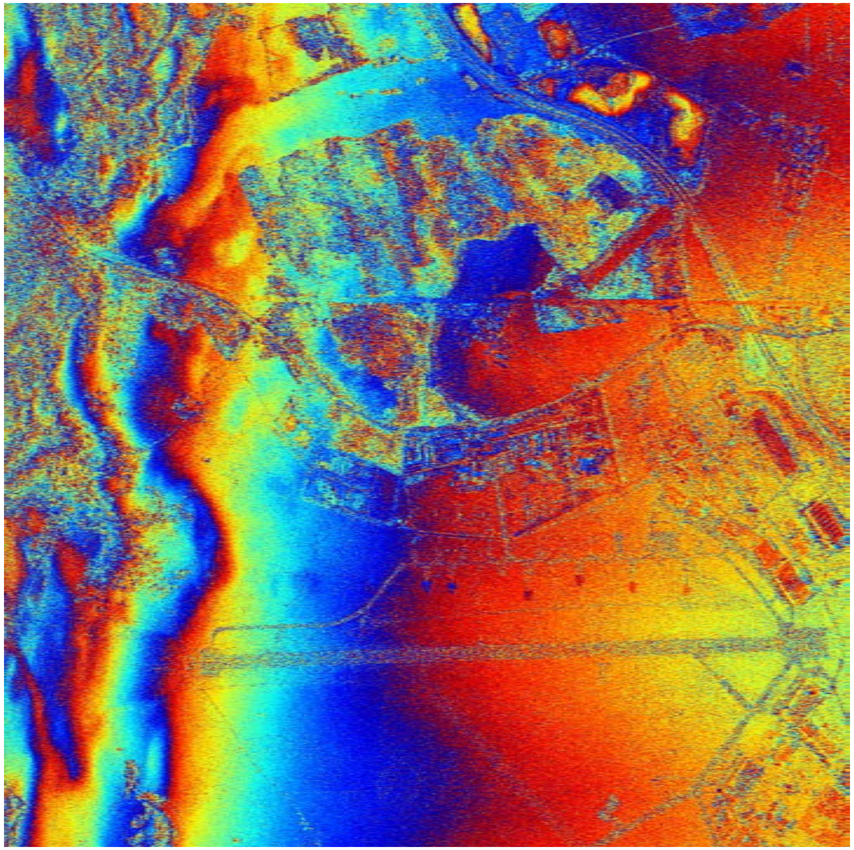

DLR E-SAR L Band
In-Pol SAR (1.5m x 3m) – Baseline 5m

↓ **POL-SAR INFORMATION**

↓ **IN-SAR INFORMATION** γ

D.E.M GENERATION

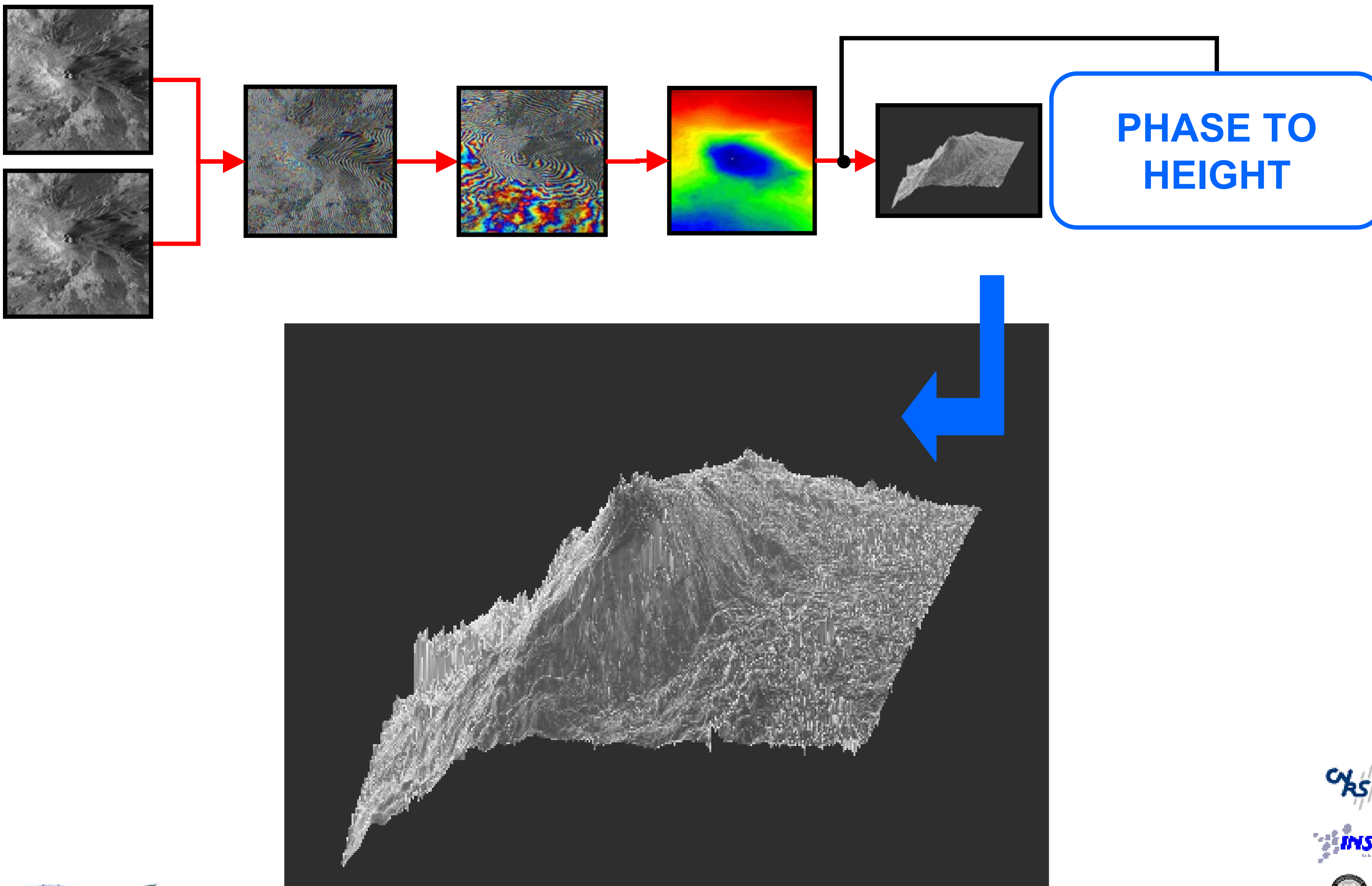

INTERFEROMETRIC COHERENCES SPECTRUM

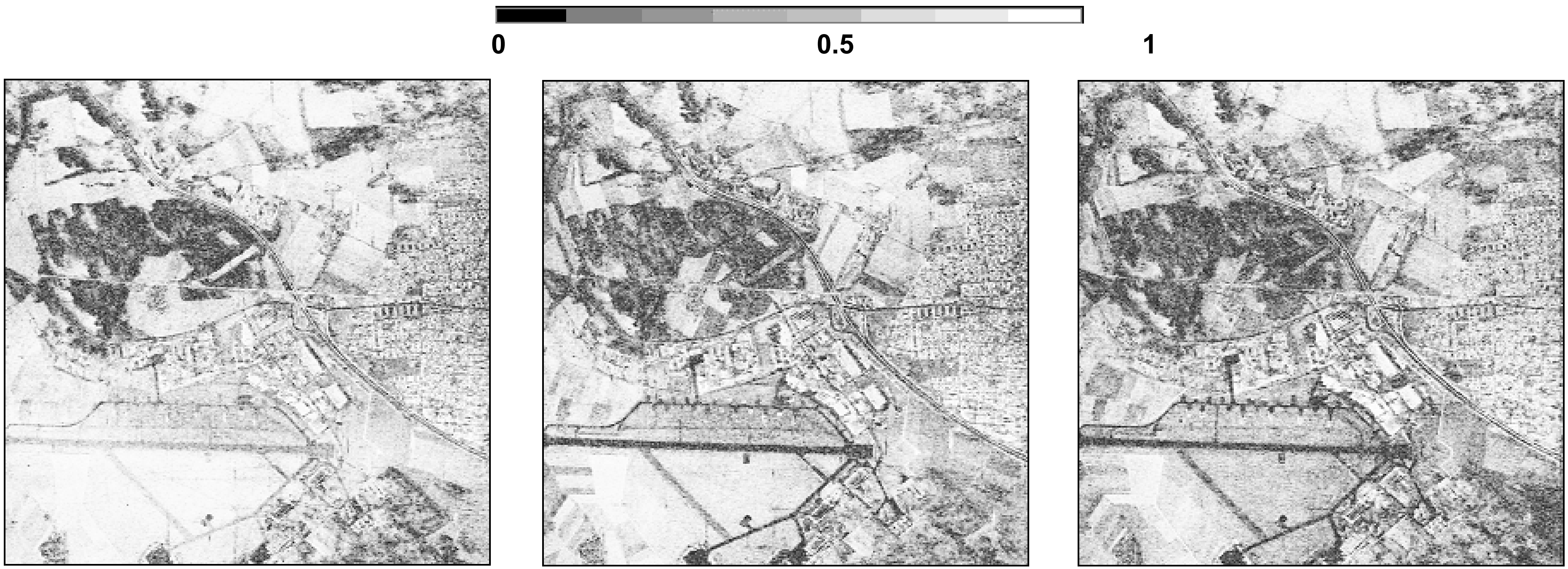

$\gamma_{HH_1-HH_2}$ $\Rightarrow$ $\underline{w}_1 = \underline{w}_2 = \frac{1}{\sqrt{2}}\begin{bmatrix} 1 \\ 1 \\ 0 \end{bmatrix}$

$\gamma_{HV_1-HV_2}$ $\Rightarrow$ $\underline{w}_1 = \underline{w}_2 = \begin{bmatrix} 0 \\ 0 \\ \sqrt{2} \end{bmatrix}$

$\gamma_{VV_1-VV_2}$ $\Rightarrow$ $\underline{w}_1 = \underline{w}_2 = \frac{1}{\sqrt{2}}\begin{bmatrix} 1 \\ -1 \\ 0 \end{bmatrix}$

$$\gamma = \gamma_{SNR} \cdot \gamma_{spatial} \cdot \gamma_{temporal} \cdot \gamma_{polar}$$

INTERFEROMETRIC COHERENCES SPECTRUM

$$\gamma(\underline{w}_1,\underline{w}_2)=\frac{\langle I_1 I_2^*\rangle}{\sqrt{\langle I_1 I_1^*\rangle\langle I_2 I_2^*\rangle}}=\frac{\langle \underline{w}_1[\Omega_{12}]\underline{w}_2^{T*}\rangle}{\sqrt{\langle \underline{w}_1[T_1]\underline{w}_1^{T*}\rangle\langle \underline{w}_2[T_2]\underline{w}_2^{T*}\rangle}}$$

COMPLEX POLARIMETRIC INTERFEROMETRIC COHERENCE

QUESTION: WHICH POLARISATION COMBINATION LEADS TO THE MAXIMUM POSSIBLE INTERFEROMETRIC COHERENCE ?

POLARIMETRIC INTERFEROMETRIC COHERENCE OPTIMISATION PROCEDURE

S.R CLOUDE – K. PAPATHANASSIOU (1999)

POLARIMETRIC INTERFEROMETRIC COHERENCE OPTIMISATION PROCEDURE

S.R CLOUDE – K. PAPATHANASSIOU (1999)

$$[T_1]^{-1}[\Omega_{12}][T_2]^{-1}[\Omega_{12}]^{T*}\underline{w}_1 = [A][B]\underline{w}_1 = \lambda_1\lambda_2^*\underline{w}_1 = \nu\underline{w}_1$$

$$[T_2]^{-1}[\Omega_{12}]^{T*}[T_1]^{-1}[\Omega_{12}]\underline{w}_2 = [B][A]\underline{w}_2 = \lambda_1\lambda_2^*\underline{w}_2 = \nu\underline{w}_2$$

$[T_2]^{-1}[\Omega_{12}]^{T*}[T_1]^{-1}[\Omega_{12}]$ is not hermitian but $\nu = \lambda_1\lambda_2^*$ are real

⬇

3 Real Eigenvalues: $\nu_1 \geq \nu_2 \geq \nu_3 \geq 0$

3 Pairs of Eigenvectors: $\{\underline{w}_{11}, \underline{w}_{21}\}, \{\underline{w}_{12}, \underline{w}_{22}\}, \{\underline{w}_{13}, \underline{w}_{23}\}$

⬇

Optimum Coherence Values: $\gamma_i = \sqrt{\nu_i}$

Optimum Scattering Mechanisms: $\{\underline{w}_{1i}, \underline{w}_{2i}\}$

POL-IN COHERENCES SPECTRUM

PHYSICAL INTERPRETATION OF POLARIMETRIC INTERFEROMETRIC COHERENCES OPTIMISATION ALGORITHM

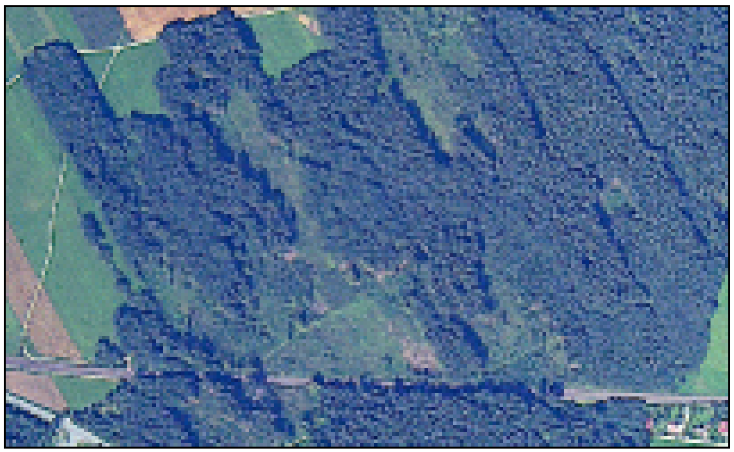

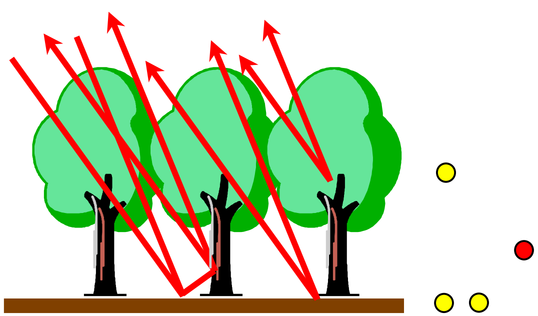

γ_{X1-X2}

$\{\underline{w}_{11}, \underline{w}_{21}\}$

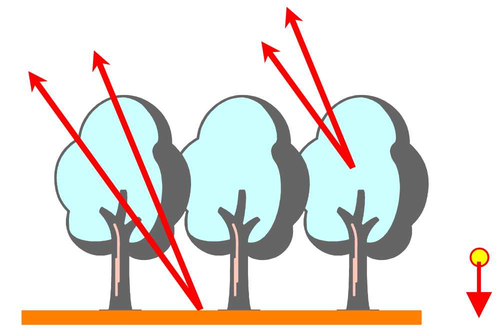

$\{\underline{w}_{12}, \underline{w}_{22}\}$

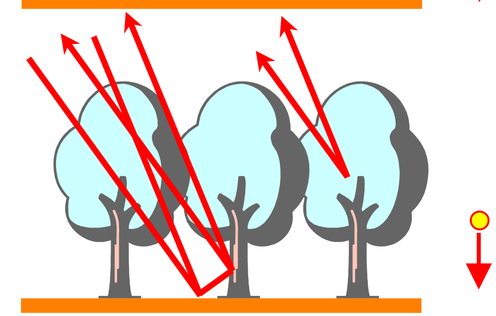

$\{\underline{w}_{13}, \underline{w}_{23}\}$

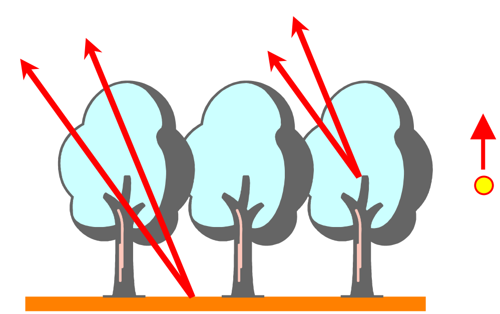

IN AN OPTIMISED WORLD

INTERFEROMETRIC COHERENCES SPECTRUM

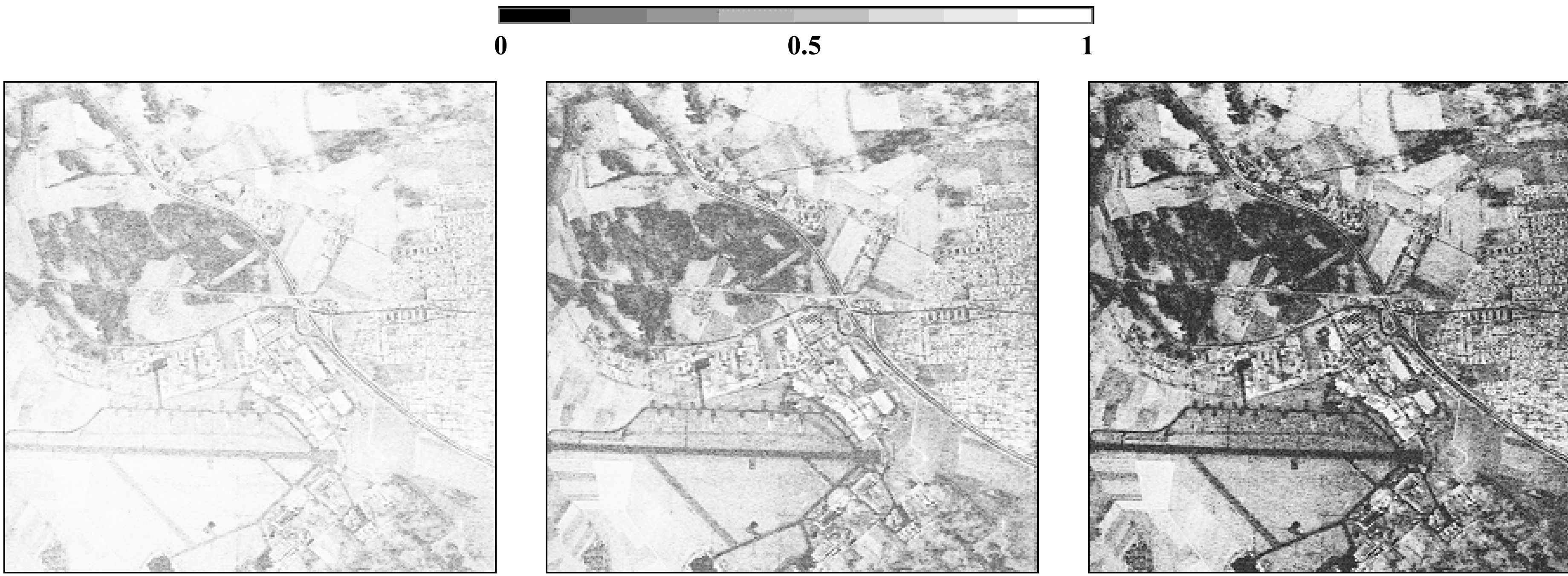

$\gamma_{opt\,1}$ $\gamma_{opt\,2}$ $\gamma_{opt\,3}$

$\Downarrow$ $\Downarrow$ $\Downarrow$

$\{\underline{w}_{11}, \underline{w}_{21}\}$ $\{\underline{w}_{12}, \underline{w}_{22}\}$ $\{\underline{w}_{13}, \underline{w}_{23}\}$

Optimum coherences spectrum $(\gamma_{opt\,1}, \gamma_{opt\,2}, \gamma_{opt\,3})$

Independent of the radar polarization basis

INTERFEROMETRIC COHERENCES SPECTRUM

$|\gamma_{opt1}|$ $|\gamma_{opt2}|$ $|\gamma_{opt3}|$

$2A_0$ $B_0 + B$ $B_0 - B$

INTERFEROMETRIC COHERENCES SPECTRUM

$|\gamma_{opt1}|$ $|\gamma_{opt2}|$ $|\gamma_{opt3}|$

Wishart H-A-$\underline{\alpha}$ segmentation

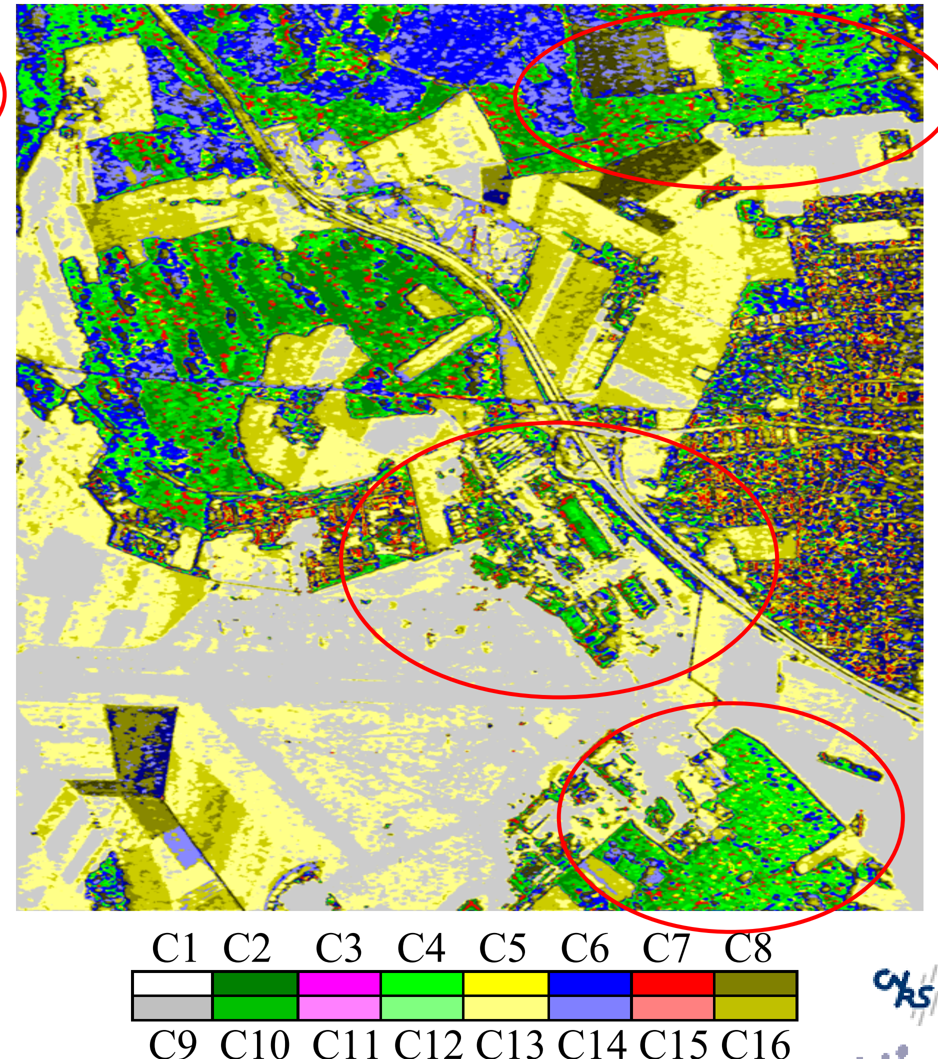

ANALYSIS OF THE OPTIMUM COHERENCES SPECTRUM

⬇

INTERFEROMETRIC COHERENCES SPECTRUM SEGMENTATION PROCEDURE

Information about the coherent scattering mechanisms

SPECTRUM DESCRIPTORS

$$A_1 = \frac{\tilde{\gamma}_{opt\ 1} - \tilde{\gamma}_{opt\ 2}}{\tilde{\gamma}_{opt\ 1}} \qquad A_2 = \frac{\tilde{\gamma}_{opt\ 1} - \tilde{\gamma}_{opt\ 3}}{\tilde{\gamma}_{opt\ 1}}$$

With : $\tilde{\gamma}_{opt\ i} = \frac{\left|\gamma_{opt\ i}\right|}{\sum_{j=1}^{3}\left|\gamma_{opt\ j}\right|}$

INTERFEROMETRIC COHERENCES SPECTRUM SEGMENTATION RESULTS

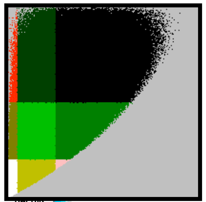

9 potential classes

COHERENCES SPECTRUM DISTRIBUTION IN THE A1/A2 PLANE

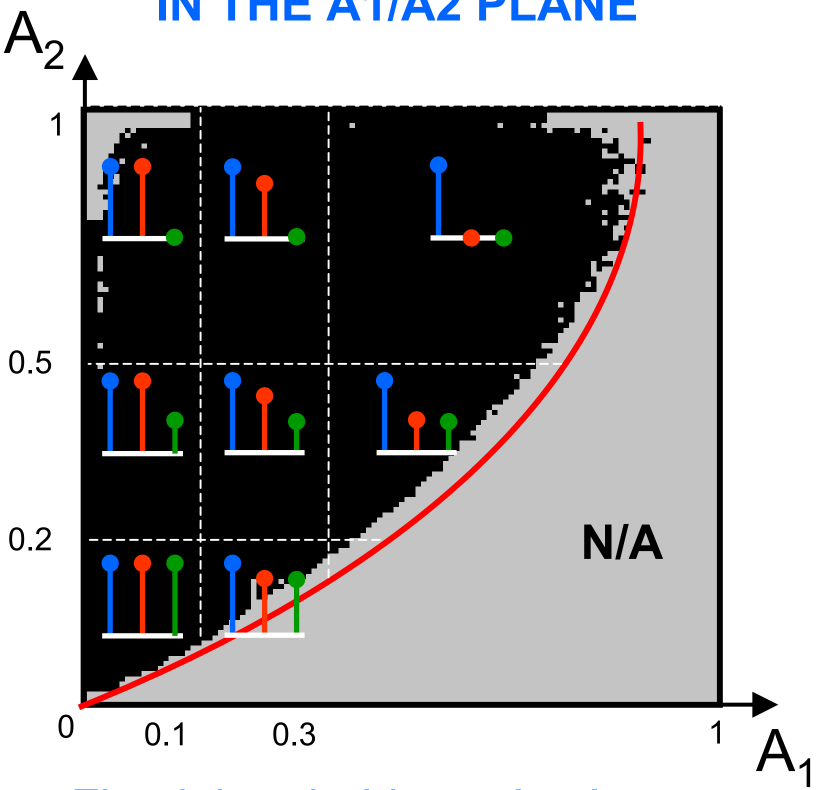

Fixed thresholds on A_1, A_2

⇓

Interpretation of the spectrum distribution

Number of coherent mechanisms

POLINSAR CLASSIFICATION PROCEDURE

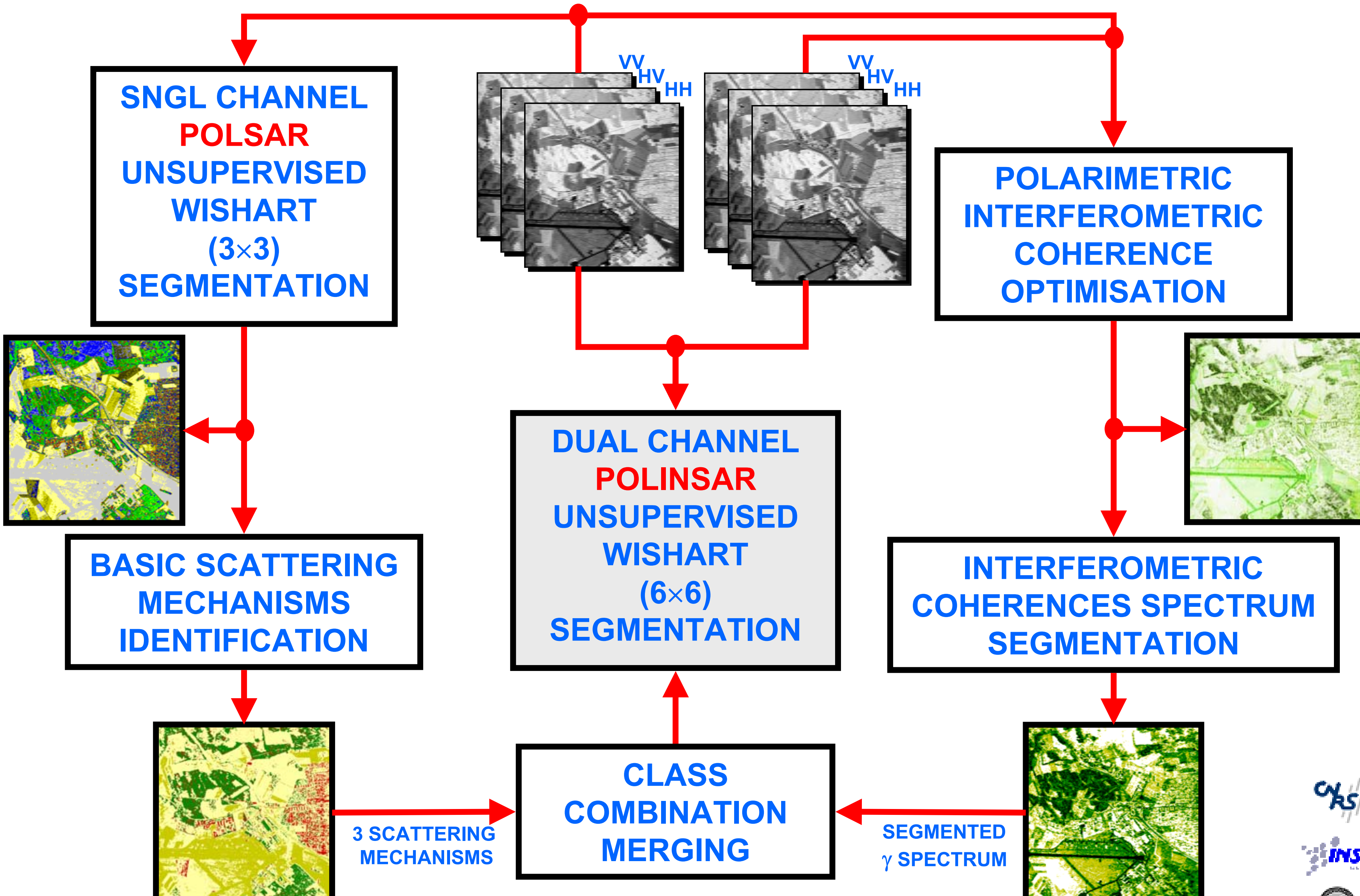

 E. Pottier, L. Ferro-Famil (01/2004)

SEGMENTATION OF EACH BASIC SCATTERING MECHANISM TYPE

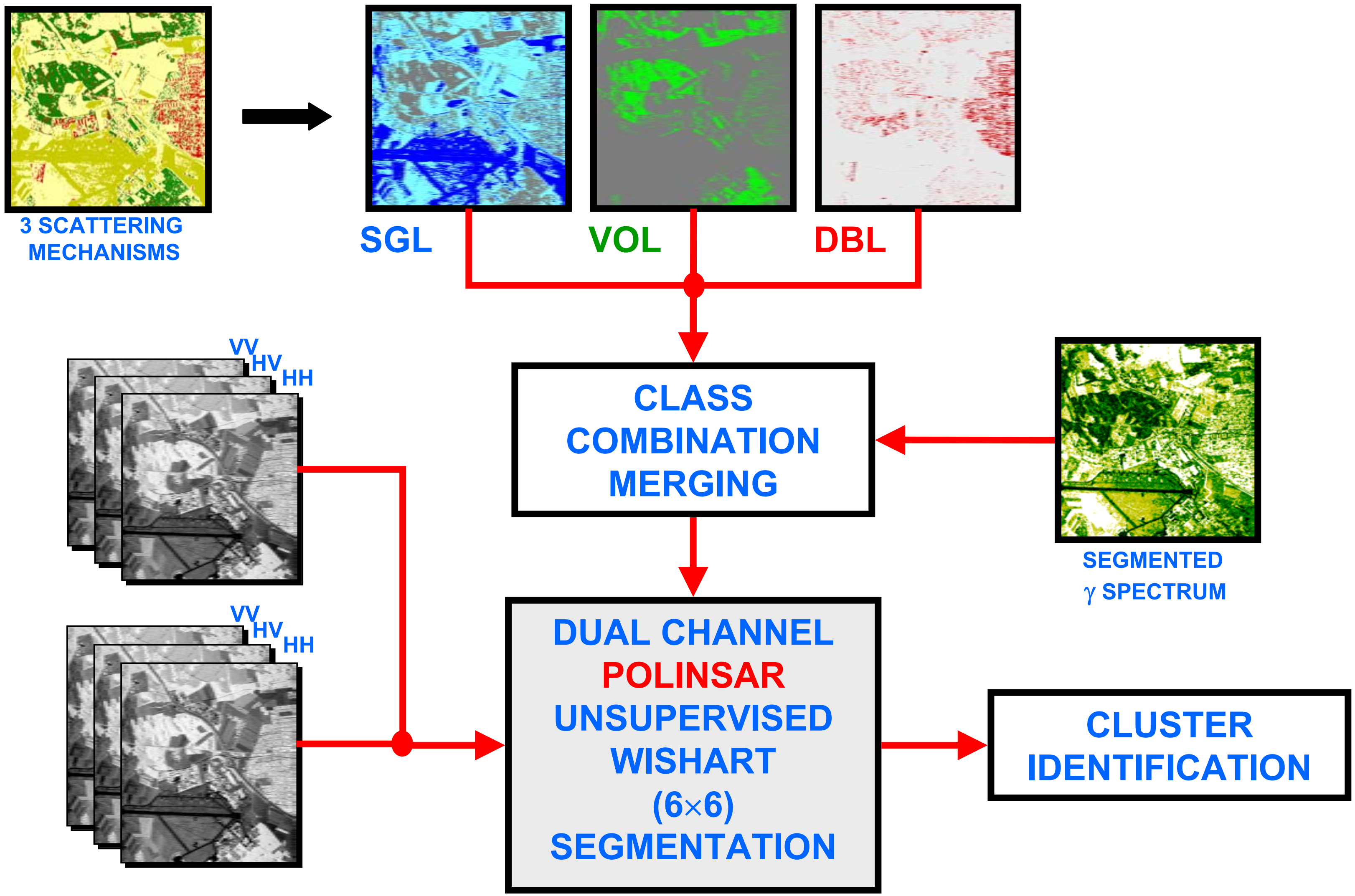

COMPLEX WISHART DISTRIBUTION

DUAL CHANNELS POLINSAR UNSUPERVISED SEGMENTATION

$$\langle [T_6] \rangle = \langle \underline{\underline{k}} \cdot \underline{\underline{k}}^{T*} \rangle = \begin{bmatrix} \langle \underline{k}_1 \cdot \underline{k}_1^{T*} \rangle & \langle \underline{k}_1 \cdot \underline{k}_2^{T*} \rangle \\ \langle \underline{k}_2 \cdot \underline{k}_1^{T*} \rangle & \langle \underline{k}_2 \cdot \underline{k}_2^{T*} \rangle \end{bmatrix} = \begin{bmatrix} \langle [T_1] \rangle & \langle [\Omega_{12}] \rangle \\ \langle [\Omega_{12}]^{T*} \rangle & \langle [T_2] \rangle \end{bmatrix}$$

POLARIMETRIC INTERFEROMETRIC COHERENCY MATRIX (6x6)

$\langle [T_6] \rangle$ FOLLOWS A WISHART DISTRIBUTION

$$P\left(\langle [T_6] \rangle / [\Sigma_m]\right) = \frac{\left|\langle [T_6] \rangle\right|^{L-p} exp\left(-tr\left([\Sigma_m]^{-1} \langle [T_6] \rangle\right)\right)}{K(L,p)\left|[\Sigma_m]\right|^{L}} = W_C\left(L, [\Sigma_m]\right)$$

L: Number of Look

p: Polarimetric Dimension

With: $K(L,p) = \frac{\pi^{\frac{p(p-1)}{2}}}{L^{Lp}} \Gamma(L) \ldots \Gamma(L-p+1)$

$[\Sigma m]$: Cluster Center of the class *m*

BAYES MAXIMUM LIKELIHOOD CLASSIFICATION PROCEDURE

$$\langle [T_6] \rangle \in [\Sigma_m] \quad \text{if} \quad d_m(\langle [T_6] \rangle) < d_j(\langle [T_6] \rangle) \quad \forall\, j \neq m$$

With: $$d(\langle [T_6] \rangle, [\Sigma_m]) = \ln |[\Sigma_m]| + tr\left([\Sigma_m]^{-1} \langle [T_6] \rangle\right)$$

$[\Sigma_m]$: Cluster Center of the class *m*

Where: $$|[\Sigma_m]| = |[\Sigma_2]|\,|[\Sigma_1']|$$

$$\begin{aligned} tr\left([\Sigma_m]^{-1}\langle [T_6]\rangle\right) = \; & tr\left([\Sigma_1']^{-1}\langle [T_1']\rangle\right) + tr\left([\Sigma_2]^{-1}\langle [T_2]\rangle\right) \\ & + tr\Big([\Sigma_1']^{-1}\left(\langle [T_{12}]\rangle - [\Sigma_{12}][\Sigma_2]^{-1}\langle [T_2]\rangle\right)\ldots \\ & \ldots \times \langle [T_2]\rangle^{-1}\left(\langle [T_{12}]\rangle - [\Sigma_{12}][\Sigma_2]^{-1}\langle [T_2]\rangle\right)^{T*}\Big) \end{aligned}$$

And: $$[\Sigma_1'] = [\Sigma_1] - [\Sigma_{12}][\Sigma_2]^{-1}[\Sigma_{12}]^{T*}$$

$$\langle [T_1'] \rangle = \langle [T_1] \rangle - \langle [T_{12}] \rangle \langle [T_2] \rangle^{-1} \langle [T_{12}] \rangle^{T*}$$

VOLUME SCATTERING MECHANISM

VOLUME Scattering Mechanism Type

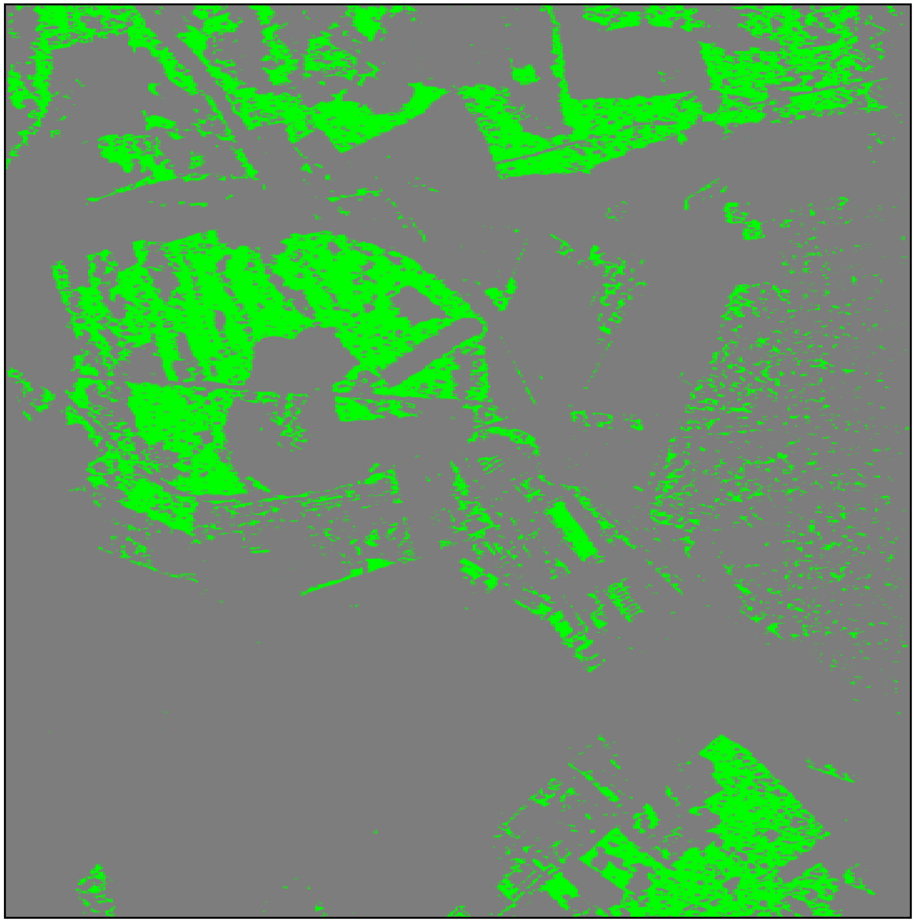

POL-IN-SAR Classification Results

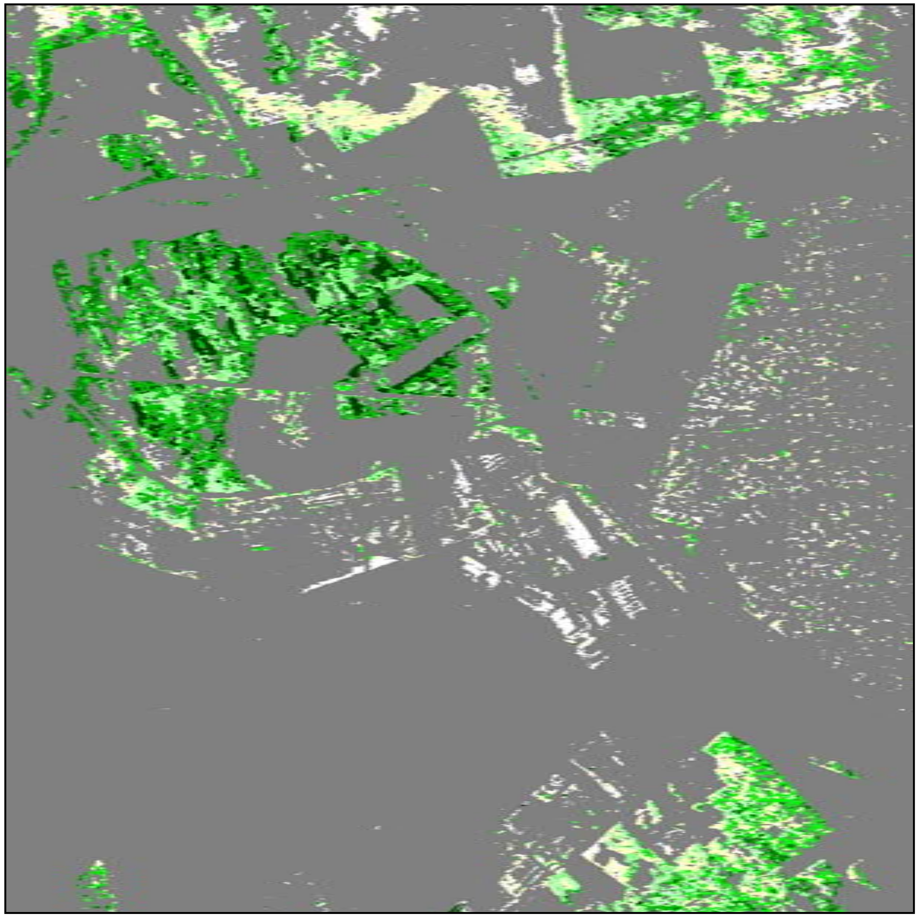

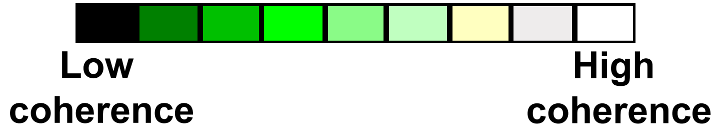

CLASSIFICATION DETAILS: FORESTED AREAS

Optical Image

POLSAR Image

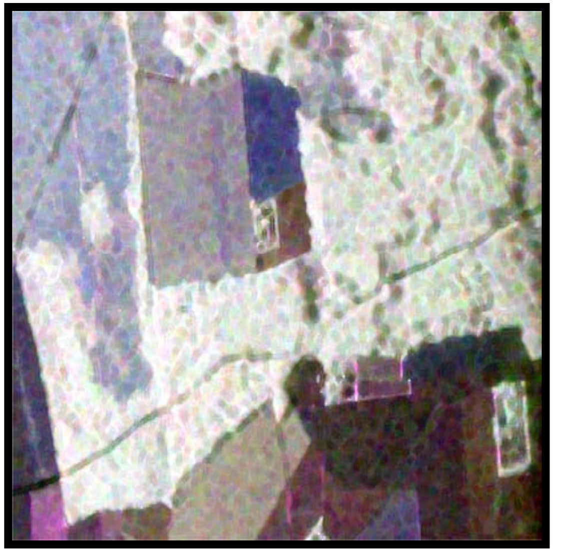

POLSAR Segmentation

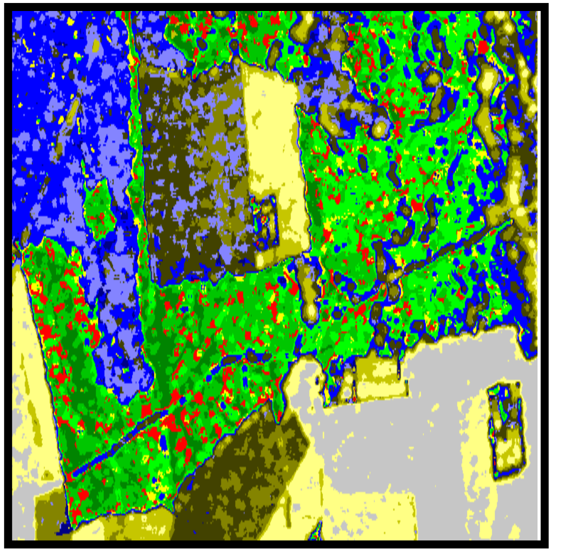

INSAR Image

VOL POLINSAR Segmentation

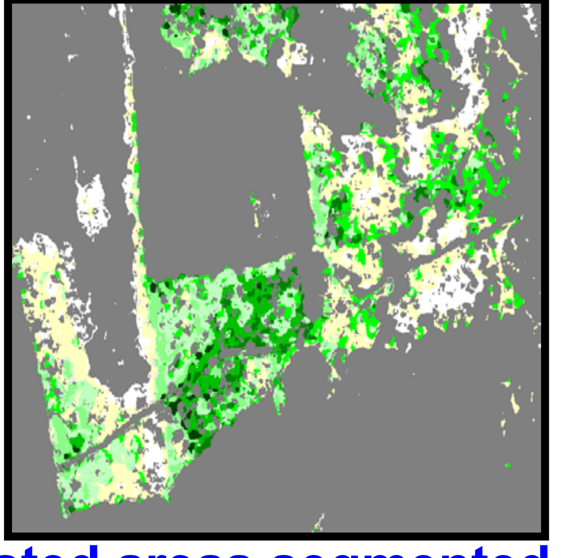

POLINSAR Segmentation

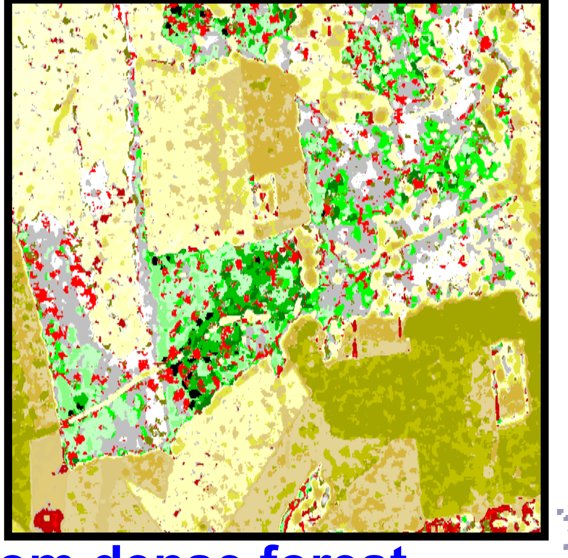

Low density forested areas segmented from dense forest

CLASSIFICATION DETAILS: BUILDINGS AREAS

Optical Image

POLSAR Image

POLSAR Segmentation

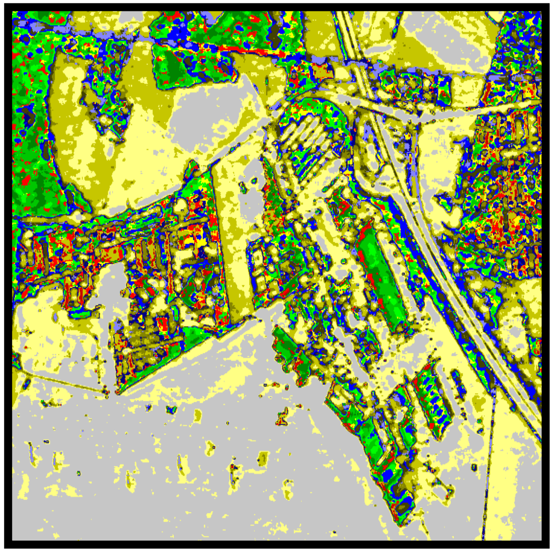

INSAR Image

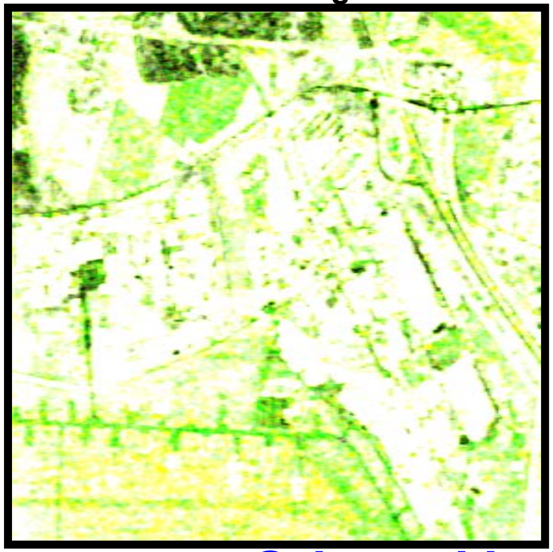

VOL POLINSAR Segmentation

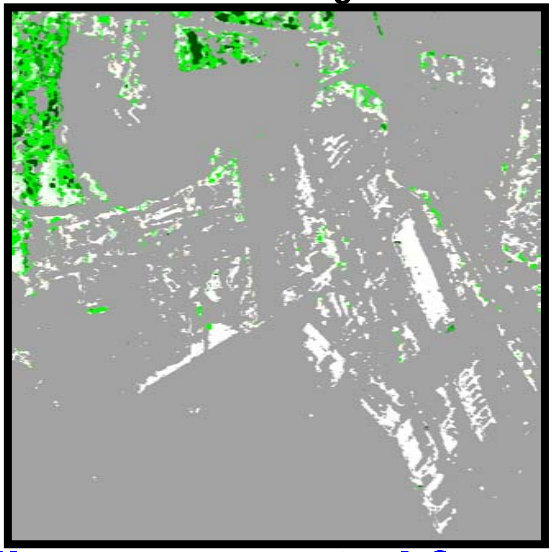

POLINSAR Segmentation

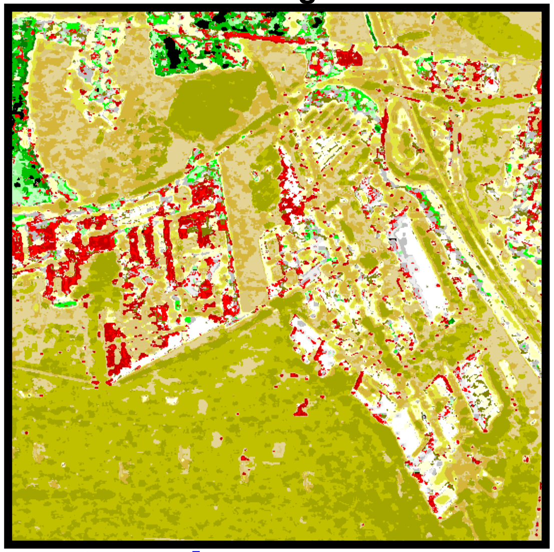

Oriented buildings segmented from vegetated areas

SURFACE SCATTERING MECHANISM

SURFACE Scattering Mechanism Type

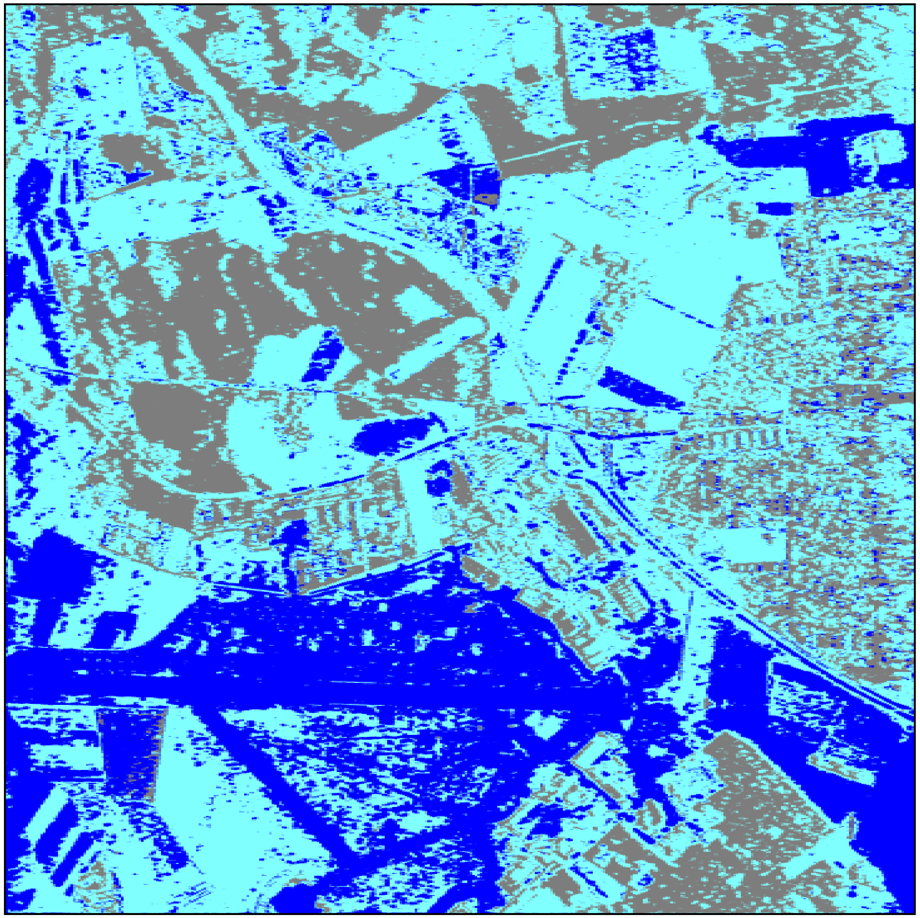

POL-IN-SAR Classification Results

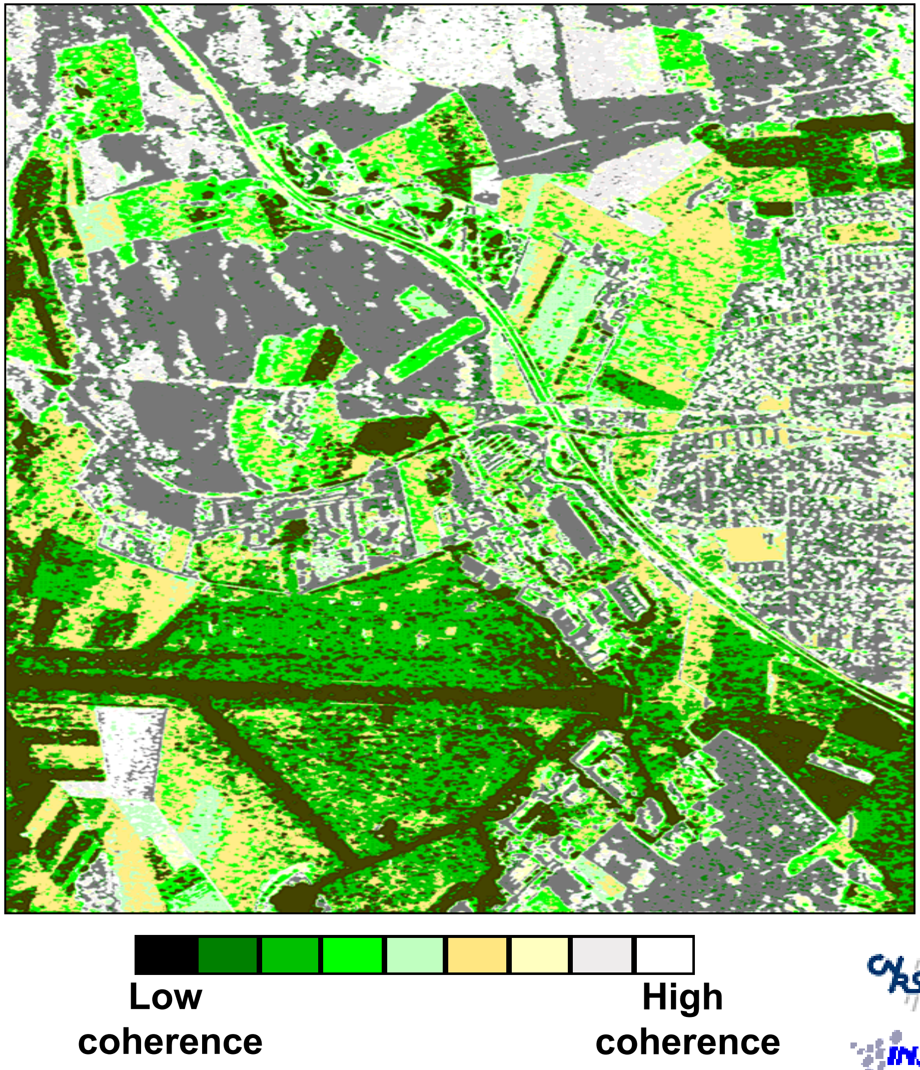

CLASSIFICATION DETAILS: SURFACE AREAS

Optical Image

POLSAR Image

POLSAR Segmentation

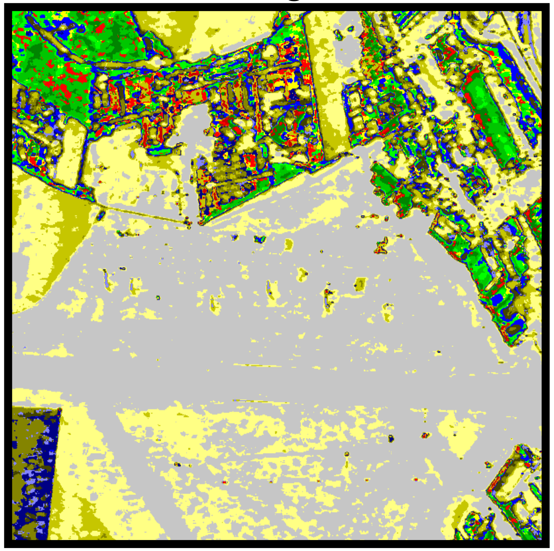

INSAR Image

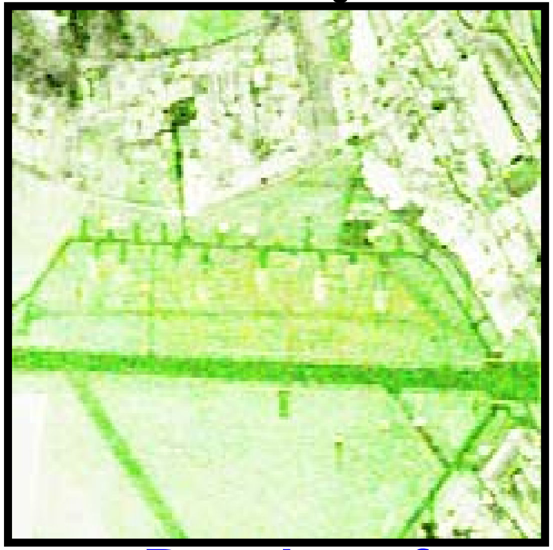

DBL POLINSAR Segmentation

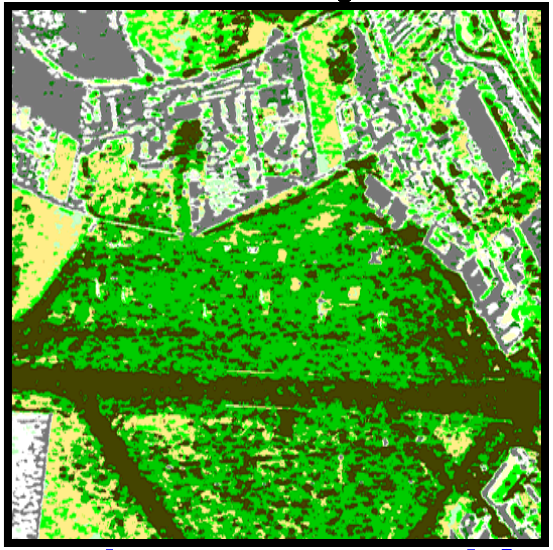

POLINSAR Segmentation

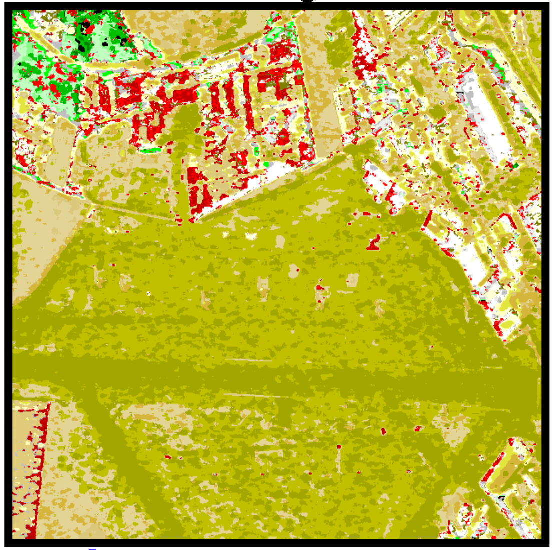

Rough surface scattering segmented from noisy areas

POL-IN-SAR CLASSIFICATION

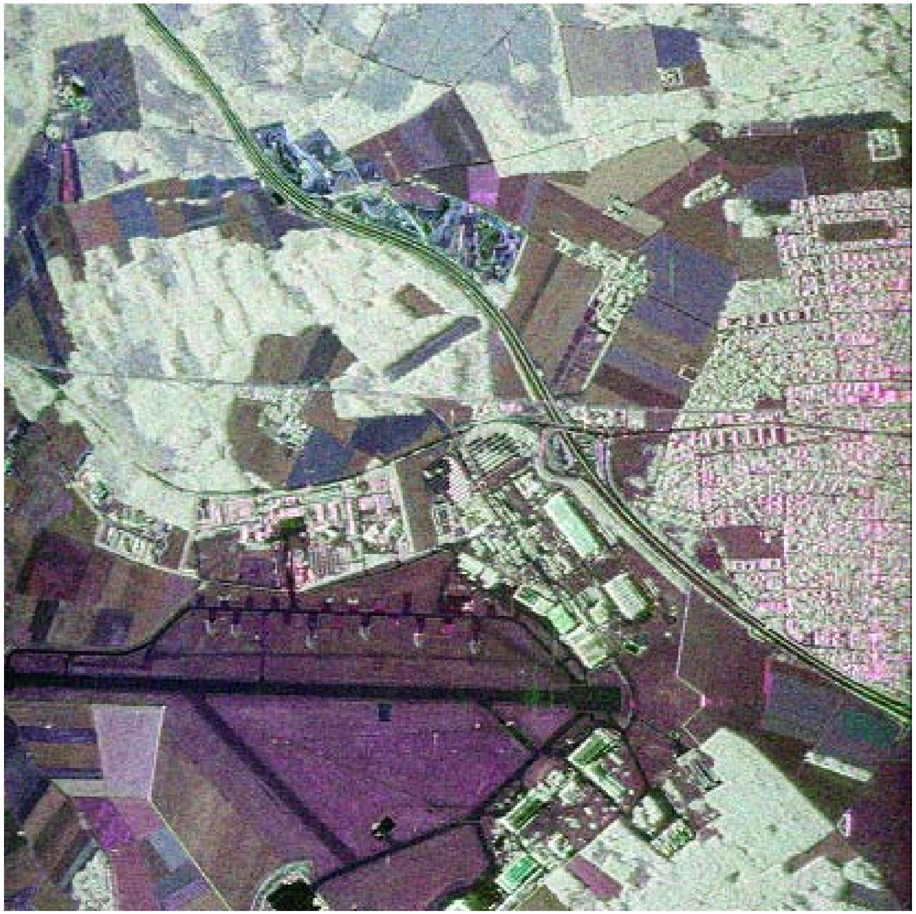

$2A_0$ $B_0 + B$ $B_0 - B$

POL-IN-SAR Classification Results

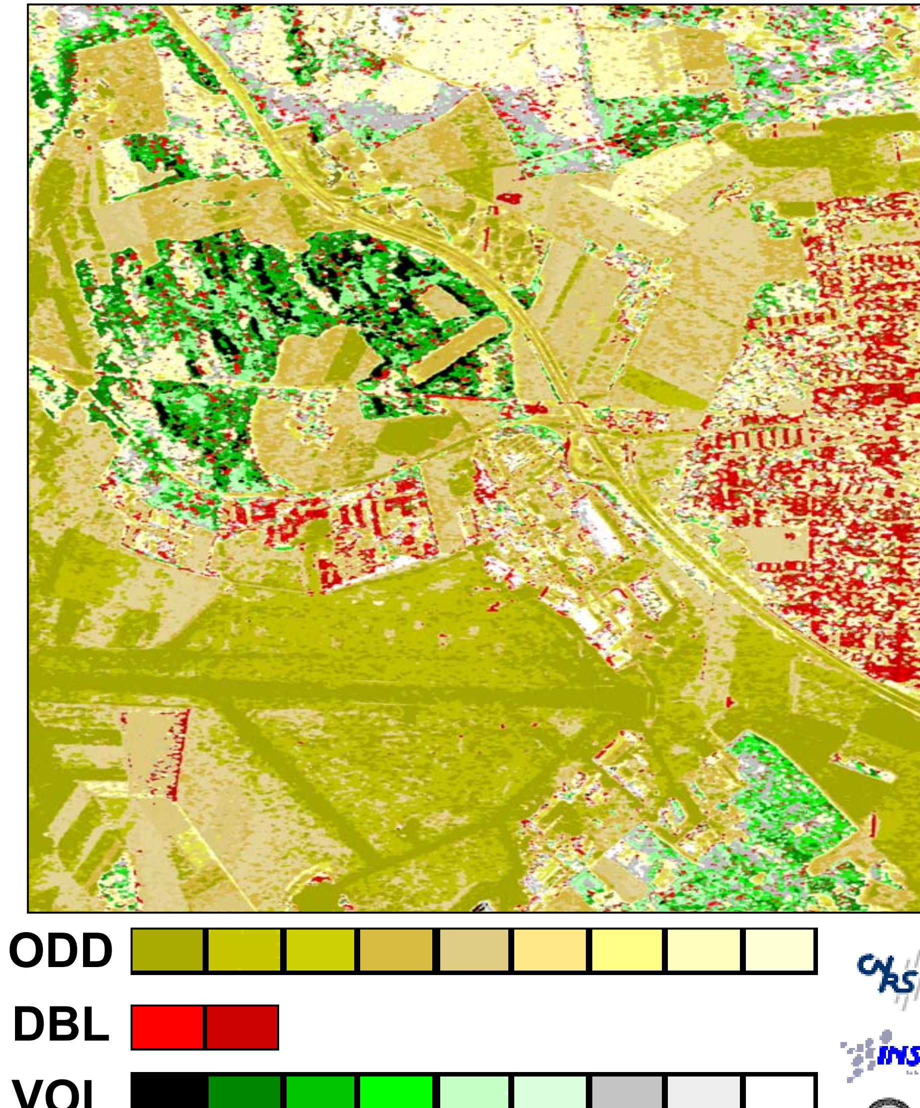

CONCLUSION

POLARIMETRIC CLASSIFICATION PROCEDURE

- Unsupervised Wishart H - A - $\underline{\alpha}$ segmentation procedure
- Identification of the basic scattering mechanisms

POLARIMETRIC INTERFEROMETRIC CLASSIFICATION PROCEDURE

- Segmentation of the optimum coherence spectrum
- Unsupervised 6 x 6 Wishart H - A - $\underline{\alpha}$ segmentation procedure

MERGING OF INTERFEROMETRIC AND POLARIMETRIC INFORMATION

⬇

COMPLEMENTARITY AND MUTUAL CORRECTIONS

FOREST HEIGHT ESTIMATION

E-SAR / Test Site: Oberpfafenhoffen

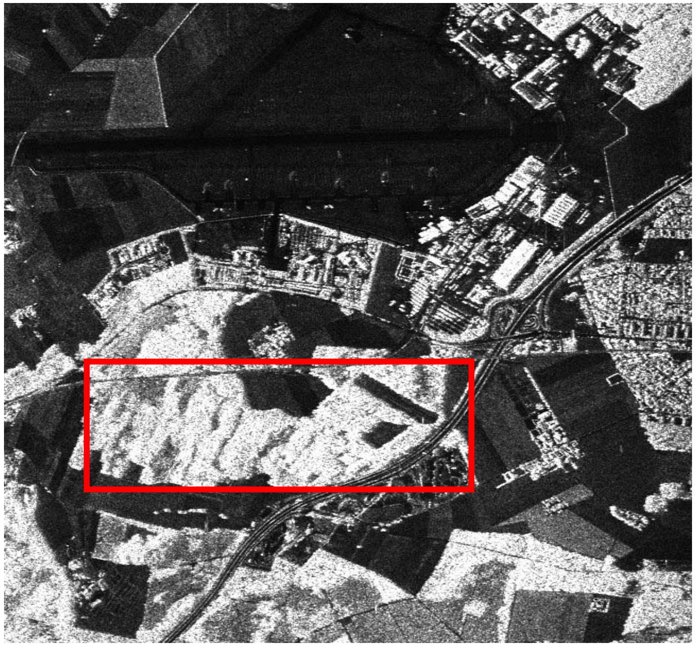

INTERFEROMETRIC
POLARIMETRIC
INVERSION

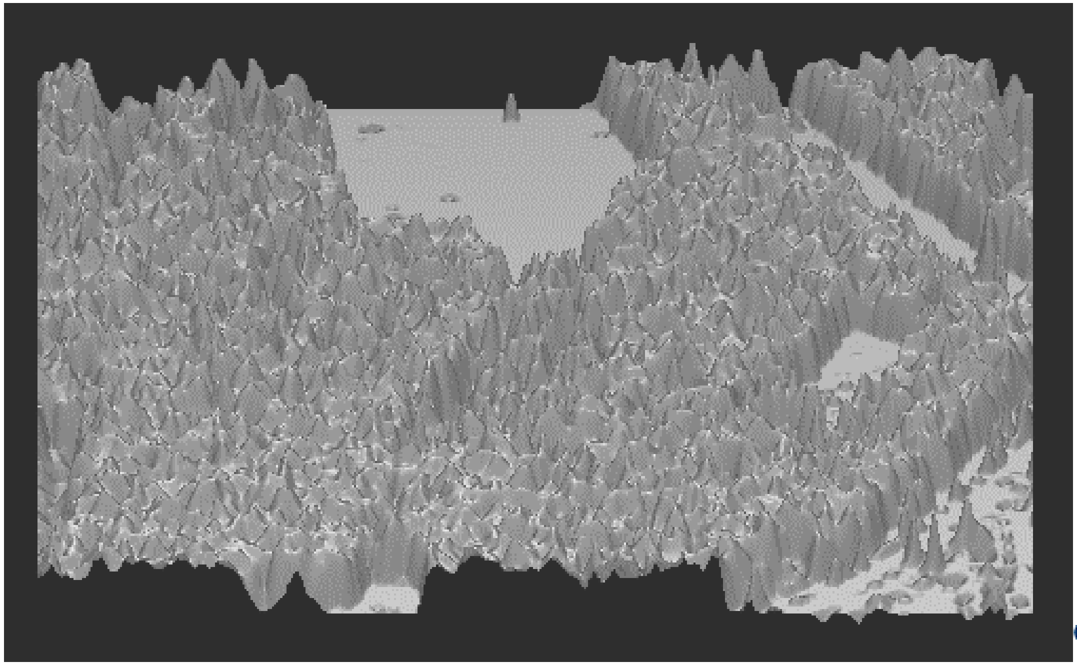

3-Dimensional Forest Height Representation

Courtesy of Dr S.R. CLOUDE and Dr K. PAPATHANASSIOU

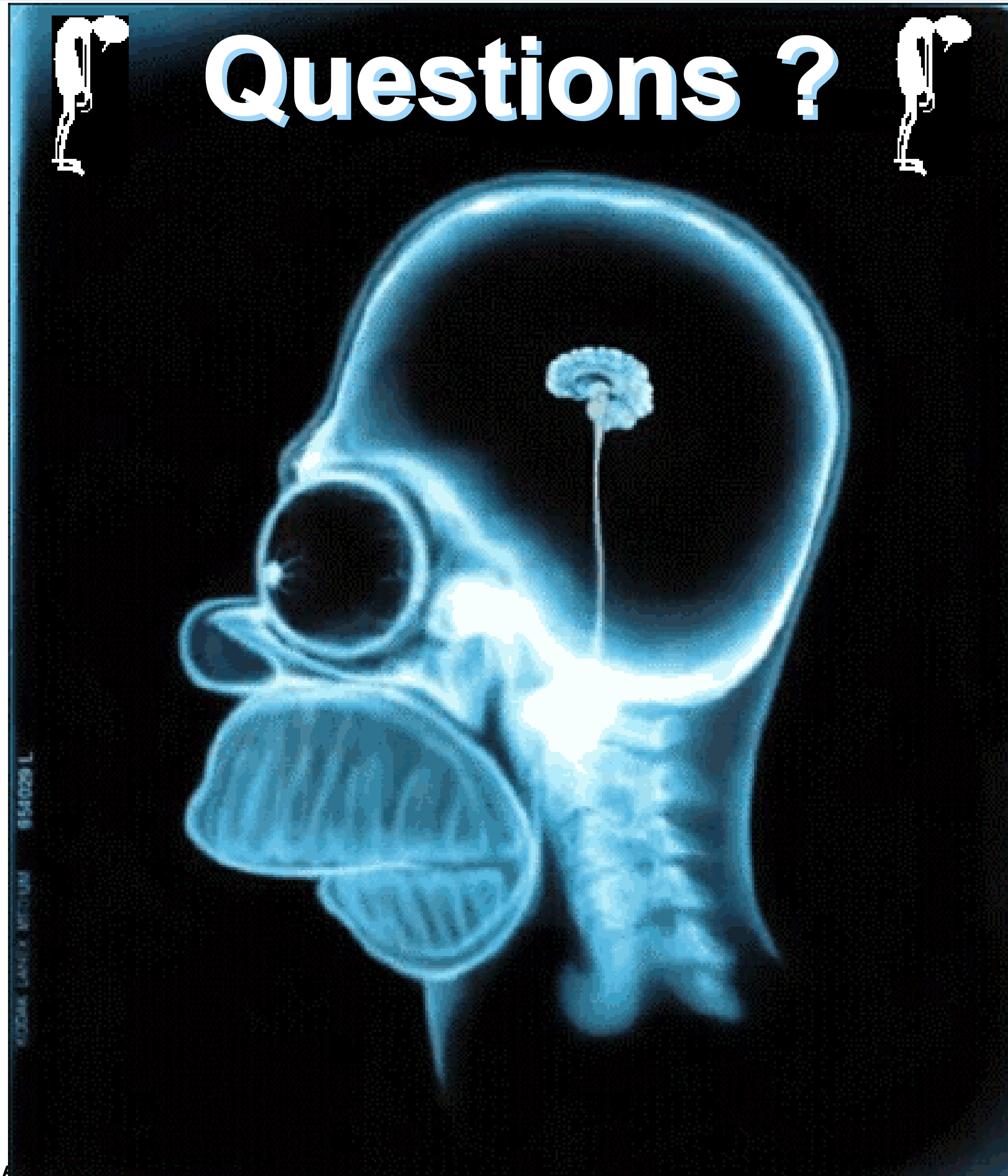
Questions ?